Comparison of damping properties for three different mooring arrangements

A.W.Vickers and L. Johanning

Camborne School of Mines
Exeter University
Tremough Campus
TR10 9EZ,United Kingdom
E-mail: a.w.vickers@ex.ac.uk and l.johanning@ex.ac.uk

Abstract

For the safe operation of floating wave energy converters (WEC's) it is required to obtain deeper understanding of the moored device as a coupled system. The motion of a WEC is dependent on the stiffness, mass and the damping characteristics of the body and the mooring system, as well as influenced by the power take of system. In order to understand the effect of the individual contributions to the coupled system, the influence of the individual parameters needs to be understood. Typical offshore oil and gas installations, in moderate water depths, are often moored using catenary configurations within linear load-extension characteristics. In many applications the damping contribution due to the mooring system is within a linear regime and hence can be applied in a linear fashion. Earlier investigation relating to mooring damping and stiffness can be found in [1-6]

Due to their physical size and the wish to install the WEC in an energetic environment, there is an increased risk that the moor will be operating in a load-extension range with non-linear characteristics. Furthermore, it is likely that for the station keeping of WECs compliant configurations are used with fibre rope sections. These would have an effect on the stiffness and damping characteristic of the mooring system [7, 8], which could importantly affect the coupled motion of a moored WEC device. The effect towards the power conversion and/or ultimate peak loads needs to be understood to allow for a safe station keeping that does not adversely affect the energy conversion.

A detailed investigation of mooring line stiffness and damping properties has been conducted at large scale tests in the Scapa Flow at Orkney. Three different mooring arrangements namely, compliant chain, compliant hybrid and nylon rope s-shape were investigated. Preliminary analysis was presented to indentify the stiffness characteristics for these large scale mooring tests in open sea environment [9]. This publication presents the continuation of the study by the second author analysing outstanding data from the Scapa Flow test series [9,10,11]. .Within the analysis presented here the main focus will be given to the energy dissipation (damping), comparing the different arrangements using the 'indicator-diagram method'. The intention of this study is to identify the damping properties of the individual mooring arrangements in order to provide information towards the analysis of a coupled system.

The outcome will present the dissipated energy (damping) results for the tests and will relate them to the preliminary stiffness analysis. This will then be used to discuss the suitability of these mooring arrangements with respect to the requirements of different WEC devices. It is also hoped to provide further information on the variability of the damping as a result of a change in frequency characteristics.

Keywords: Mooring damping, Wave Energy Converter, Large scale testing,

Nomenclature

T_0	=	Pre-tension
T_h	=	Horizontal Tension
T_x	=	Tension in the x-direction
T_y	=	Tension in the y-direction
ω_{ratio}	=	Frequency ratio
ω_f	=	Forced oscillation frequency
ω_n	=	Natural oscillation frequency
h	=	Water depth

a = Amplitude
E = Dissipated energy (Damping)
w = Weight per unit length

1 Introduction

As the wave energy industry grows it is coming ever closer to the deployment of competitive wave energy farms. Up to this point the installation of wave devices has been a novel and project specific event installing a single device for short periods of time with the exception of the Pelamis array in Portugal. Wave energy array layouts will be required to enable economical energy conversion. There is currently very little practical experience in installing multiple devices and safe station keeping will be one of the major requirements. Current experience from offshore installations for the oil and gas industry can not be directly transferred to the offshore energy industry since the operating modes of the WEC devices, the water depth and sea states into which they will be deployed can be significantly different.

Economical considerations for marine energy installations will most likely result in densely packed array formations. This requires typically a small mooring 'footprint' of each single device within the array. In order to allow for this and to avoid contact between to mooring lines the use of stiff arrangements in taut or semi-taut configurations as apposed to long catenary moorings could be suggested. Whilst these configurations are applied in the offshore oil and gas industry, the engineering challenge for the marine renewable sector will be to make such configurations perform in much shallower water. The applications of taut arrangements, like TLPs in the offshore industry, are in water depth of hundreds of meters, whilst typical marine renewable energy devices are likely to be installed in water depth of 30 to 100m.

In order to identify the station keeping characteristics for a particular mooring configuration static tension-excursion diagrams are often applied. These diagrams can be used to express the mooring stiffness contribution to the coupled system.

Figure 1a represents an example of such a diagram for a chain. This example was used by Johanning and Smith [10] highlighting the importance of the tension behaviour where the tension becomes non-linear once most of the mooring line is lifted. The work by Johanning and Smith [10] discussed the tension characteristics for three different configurations (single chain, hybrid line, nylon rope s-shape), that are re-produced in figure 1b. The presentation of the mooring characteristics in this manner allows only a preliminary study of the mooring contribution to the coupled moored system. However, in order to develop the coupled prediction of a moored system the damping properties of the floating body and its moor must also be understood.

Mooring line damping has been studied by Webster [6] using the indicator diagram method to determine the damping and stiffness of the mooring lines. This work was then taken further by Johanning et.al [7] conducting small scale tank experiments to study damping properties of a catenary chain mooring line. This work was extended by large scale experiments in the Scapa Flow at Orkney, where initial damping results for a catenary chain configuration are presented by Johanning and Smith [10,11]. The main aim of this work is to present the remaining damping results for the 'hybrid line' and the 'nylon s-shape' configuration.

2 Experimental setup

Large scale experiments with an 82t vessel moored on a 22mm single chain at a mean water depth of 24m were performed at Scapa Flow to study different mooring configurations. The tests were performed in sea conditions as shown in figure 2. An installed acoustic Doppler system measured a peak current flow of 0.15m/s during the test phase. The tests

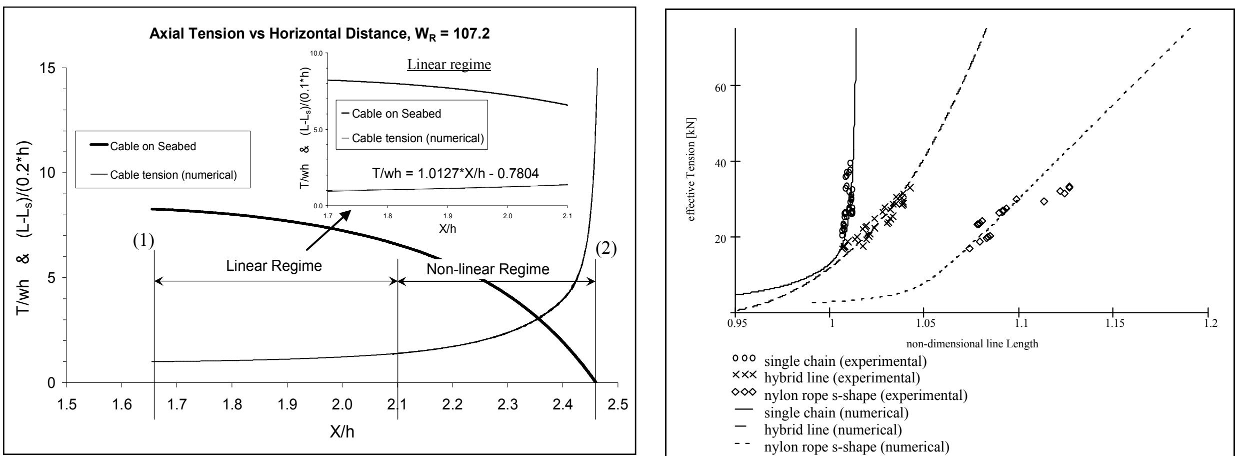

(a) (b)

Figure 1a,b (a) Indicative tension-excursion diagram for chain; (b) Comparison of tension characteristics for three different mooring configurations

Figure 2 Visual account of sea state during tests

employed a vessel with a length, breadth and displacement of 17.5m, 5.48m and 82 tones respectively. The objective of the experiments was to measure and compare the line damping of various mooring line configurations. The method used to identify the damping properties was based on an 'oscillatory' approach. For this the vessel is displaced from its equilibrium position to different pre-tensions at which oscillating surge motions are applied to measure tension characteristics. Indicator diagrams are derived from the measured tension and surge motion as described by Webster [6], and then used to identify the damping properties for the different pre-tensions. The mooring configurations applied are shown in figure 3a-c and the details of each mooring configuration are detailed in table 1. For the single chain configuration (figure 3a) a 22mm studless chain with a length of L = 80m was used. The hybrid line configuration (figure 3b) was a combination of a 38mm studless chain (L = 22.8m) towards the lower end at the seabed and a 40mm (8-Strand) nylon rope (L = 41.2m) at the upper end. The third configuration (figure 3c) was laid in a s-shape using three sections of a 40mm (8-Strand) nylon rope with a length of $L_{Line}\ A$ = 13.8m, $L_{Line}\ B$ = 10.2m and $L_{Line}\ C$ = 33.4m.

Initial preliminary tests were conducted in 2006 to establish measurement procedures suitable in real sea conditions. The improvements from these tests

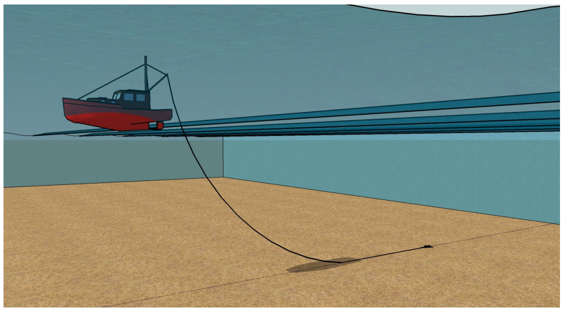

Figure 3a Catenary Chain

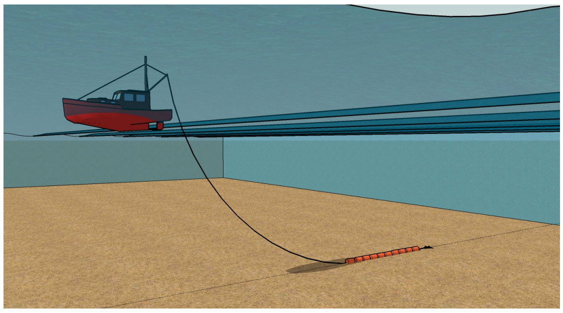

Figure 3b Chain rope hybrid

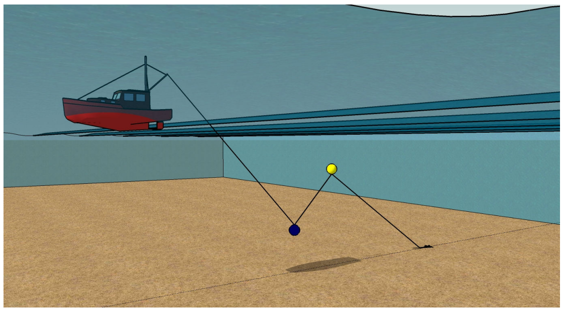

Figure 3c Floater sinker s-shape

allowed an in-depth study of the three configurations identified in figure 3a-c in 2007. A detailed discussion on the preliminary tests and in-depth study can be found in [10,11].

The main difficulty was to identify the correct position of the anchor point to establish the correct horizontal distance, from anchor point to vessel. However, this was overcome by experimental techniques discussed in [7]. Another difficulty was to obtain acceptable oscillatory surge motions around an equilibrium position due to the controllability of the vessel. In order to obtain such oscillatory motion

		Line material properties			Mooring line properties		
		22mm Studless chain	38mm Studless chain	40mm Nylon rope	Single chain	Hybrid line	Nylon Rope S-shape
Properties	Symbol[unit]	Value	Value	Value	Value	Value	Value
Maximum breaking limit	MBL[kN]	401	1159	223	401	223	223
Characteristic diameter	D[mm]	22	38	40	-	-	-
Initial line length	L[m]	80	23	41.2,33.4,13.8,10.2	80	64	57
Submerged weight	*w*[N/m]	82	245	1	82	88	4
Axial stiffness	EA[kN]	41000	123000	518	41000	803	556

Table 1 Mooring configuration properties

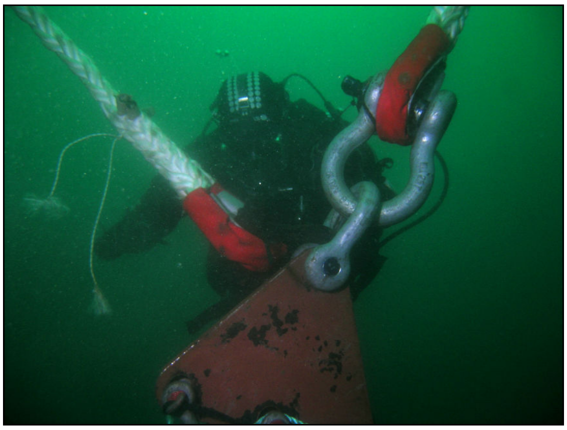

Figure 4 Visual account of 'Nylon rope S-shape' mooring configuration

it was required that the vessel was manoeuvred smoothly back and forward in a sinusoidal fashion. However, the vessel has had only a manual control and as a result the oscillatory surge motion around the equilibrium was dependent on the skills of the vessels skipper.

The installation of the mooring configuration was carried out by the research vessel and its crew by descending the anchor with the mooring configurations attached. A DGPS reading was taken at the descend of the anchor that provided an initial anchor position. The accurate location was defined using the circumference method as discussed in [7]. In addition divers were used to locate the position and provide depth reading as well as taking visual accounts (figure 3).

2.1 Transient tests

Transient test were performed to identify only the natural frequency at given pre-tensions. No attempt was made to obtain damping values from these tests since the variation in surge amplitude has a significant affect on the mooring line damping properties.

These transient tests were obtained by gently surging forward to a horizontal distance providing tension characteristics just below the pre-tension of concern, to avoid sudden snatch loads. The engine revs were then increased to the thrust associated to a specific pre-tension. Due to the initial acceleration the vessel overshot the equilibrium position associated to the pre-tension, and whilst the engine revs were held constant, a transient motion was achieved (figure 5). Different pre-tensions were investigated by varying the thrust of the vessel.

From the resulting transient graph, as shown in figure 5, natural frequencies could be identified for each specific pre-tensions. The graph in figure 5 represents the transient test for a chain-rope configuration with an associated pre-tension T_0 = 12.8kN. The measured natural period was found to be, t_n = 23.2sec. By conducting similar tests for each mooring configurations sensible frequencies could now be used for the oscillatory experiments. This knowledge could also be used to perform test below and above the natural frequency at particular pre-tensions associated to a specific configuration.

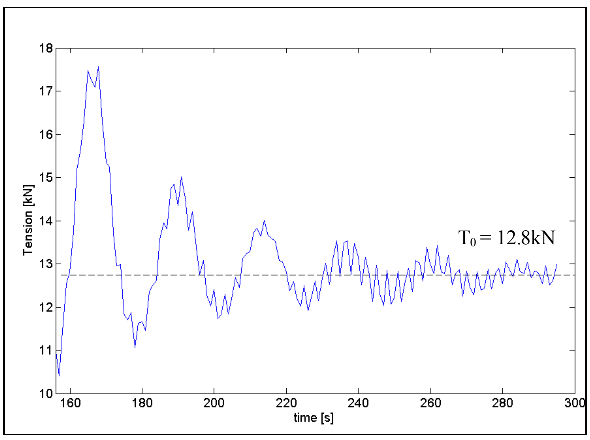

Figure 5 Example of transient test for associated pre-tension related to a thrust of 600RPM (chain-rope hybrid configuration)

2.2 Oscillatory experiments

An oscillatory method was performed to evaluate the damping effects for the different mooring configurations. The damping was measured for various pre-tensions T_0 and different surge amplitudes a, for the three mooring configurations; chain, chain-rope hybrid and nylon rope S-shape.

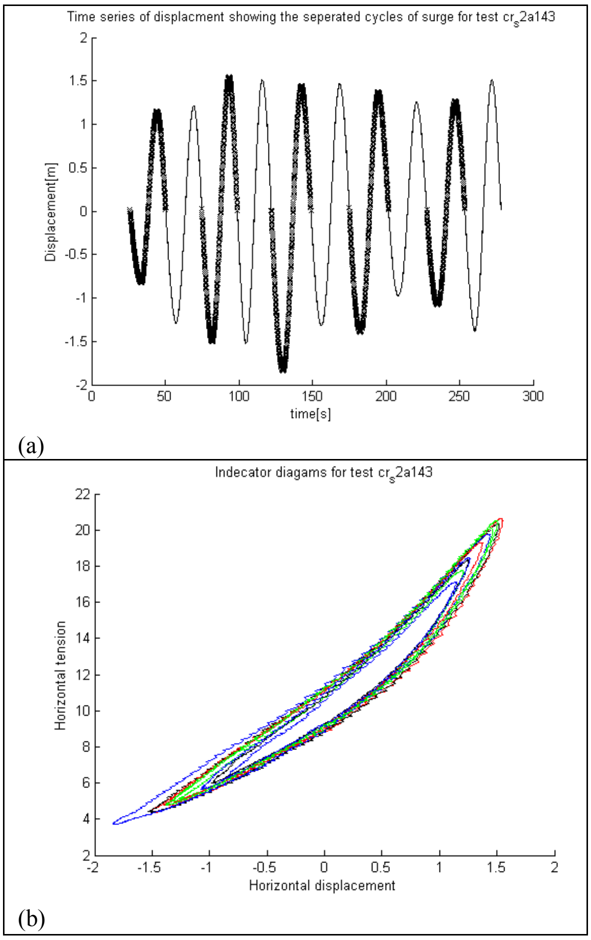

Figure 6a,b (a) time history of oscillatory surge motion, (b) resulting indicator diagrams for time history (test: cr_2a143)

Test Name	Thrust Range [RPM]	Average Surge Amplitude [m]	Pre-tension[kN]	Natural period [sec]
cr_s1n141	500-700	1.98	13.1	17.75
cr_s2n142	500-600	1.50	10.6	24.94
cr_s2a143	500-600	1.37	10.8	24.94
cr_s2b144	500-600	1.00	10.4	24.94
cr_s1n145	600-700	1.25	14.7	20.48
cr_s1b146	600-700	0.79	14.9	20.48
cr_s1b147	500-700	2.06	13.1	23.20
fs_s1n201	600-700	0.99	14.6	20.75
fs_s1n202	500-700	1.96	13.6	21.75
fs_s2n203	500-600	1.33	11.0	24.88
fs_s1a204	500-700	2.44	13.0	21.75
ch_s2a116	500-600 / 500-700	0.75/0.92	11.5/13.0	26/19.5
ch_2b117	500-700	0.95	13.4	19.5
ch_s2n115	400-600	1.88	9.4	33
ch_s2n114	500-600	1.03	10.7	26.25

Table 2 oscillatory tests properties

Within this document the tension analysis is always referring to the horizontal tension T_H and hence the pre-tension T_0 is presenting the horizontal pre-tension.

To obtain an oscillatory surge motion as shown in figure 6a, the vessel was manoeuvred about the equilibrium in a sinusoidal fashion, attempting to maintain constant surge amplitude a. The vessels control was such that changes in thrust were limited to approximate 400 to 700 rpm in steps of 100 rpm or 200rpm. The oscillatory tests properties are shown in table 2. The pre-tensions for each cycle for one sinusoidal test are defined as the average tension of the cycle, where the natural period T_n was obtained from corresponding transient pre-tension tests.

The indicator diagram method was applied as described by Webster [6] plotting the change in tension against the surge variation for one sinusoidal cycle. For these individual cycles were separated as shown in figure 6a. Figure 6b represents the resulting indicator diagrams from the time history shown in figure 6a. It can be identified that each individual indicator diagram displays a hysteresis effect with varying magnitude. Because the starting and ending point of each time history cycle is the same the indicator diagrams take the form of a closed loop. The area within a closed loop is proportional to the energy dissipation E. The mathematical expression for one sinusoidal cycle is given in the form

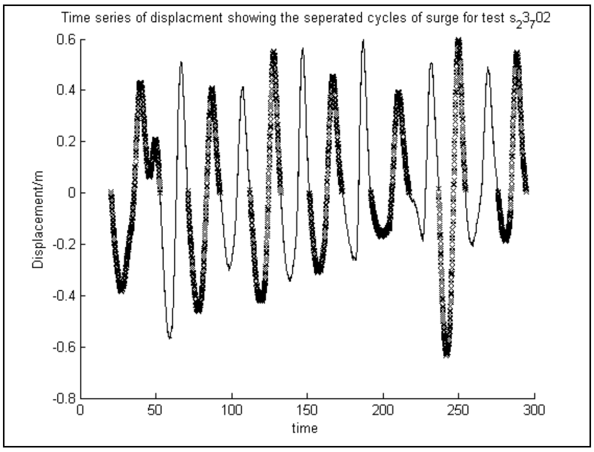

Figure 7 Oscillatory time history with large anomalies

$$E = \int_{t}^{t+T_n} T \frac{d\delta}{dt} dt , \quad (1)$$

Where T is assumed to be the tension of the mooring line during one oscillation surge cycle $d\delta/dt$.

It is worth pointing out at this stage that the hysteresis effect would be minimal or non-existing, if only a small amount or no energy would be dissipated. Such results were obtained in earlier investigations as published by Johanning and Smith [9] investigating the linear and non-linear mooring regime as indicated in figure 1a.

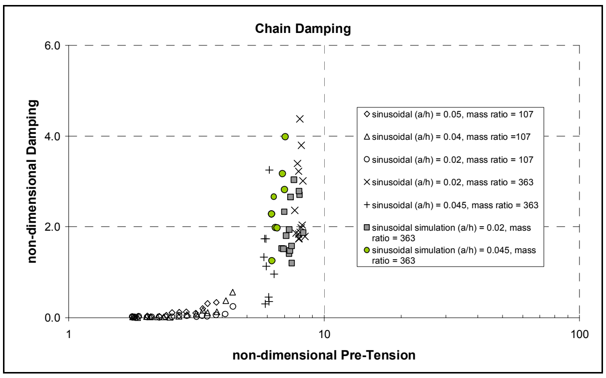

Figure 8 Chain damping for small scale and large scale experiments.

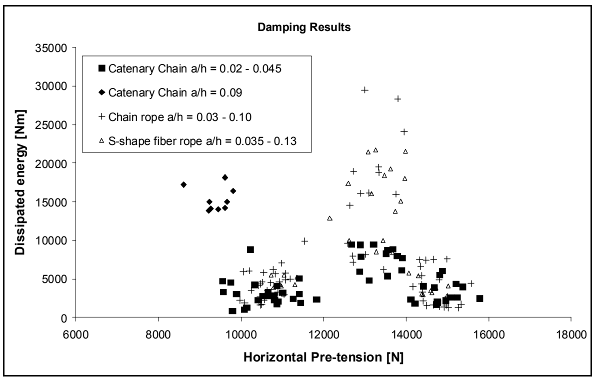

Figure 9 Dimensional damping results for all line configurations

As mentioned before the controllability of the vessel did not necessarily allow the production of regular sinusoidal motions as indicated in figure 7. This will contribute to errors in the evaluation of the damping and hence cases with large anomalies were not considered within the analysis.

3 Discussion of damping results

A preliminary damping analysis of the 2007 Scapa Flow tests, which only considered the catenary chain configuration, has been published by Johanning and Smith [11]. Within figure 8 these preliminary damping results are displayed along with small scale results as presented by Johanning et.al. [7]. Following the work by Webster [6] the damping, tension and surge amplitude are plotted in non-dimensional terms expressed in ratio's *E/awh*, *T/wh* and *a/h*, respectively. The nomination *w* is describing the submerged weight and *h* the water depth.

The results show an inherent trend of an increase in damping with increased pre-tension. Tank test result over a wider pre-tension range conducted by Webster [6] identified a Gaussian type shape indicating a peak damping followed by a decrease in damping. The results from the investigations in figure 8 [7] did not cover the wider pre-tension range and hence represents only the initial Gaussian type shape before the damping would peak.

3.1 Damping results for different configurations

In the following only the damping results from the three mooring configurations of the large scale investigation at Scapa Flow are considered. The damping results from tolerable individual sinusoidal motions for all line configurations are presented combined in physical parameters (dissipated energy *E* over pre-tension T_0) in figure 9. The comparison between the results and numerical modelling packages such as OrcaFlex has been done for the catenary chain by Johanning and Smith [12]. Comparison between the hybrid and floater sinker arrangement is of the scope for this publication but would be part of further work. The initial observation that can be made form this graph is that an increase in damping is followed by a decrease in damping with the appearance of a peak over the investigated pre-tension range. Furthermore data points for the catenary chain configuration at an average value of *a/h* = 0.09 did not follow the trend of the other results. This phenomenon could be attributed to the test circumstances where large surge amplitudes *a* were possible since this tests were performed at small pre-tension for a thrust range from 400 to 600rpm (ch_s2n115). For this test range a significant part of the mooring line was laid on the seabed at 400rpm whilst fully lifted at maximum forward thrust of 600rpm.

In figure 10a-c the damping results from figure 9 are presented in non-dimensional terms as was applied in figure 8. The different configurations are plotted individually since the non-dimensional values for the S-shape fibre rope do not match the once of the other two configurations. This is a result of difference in submerged weight per unit length *w* (see table 1).

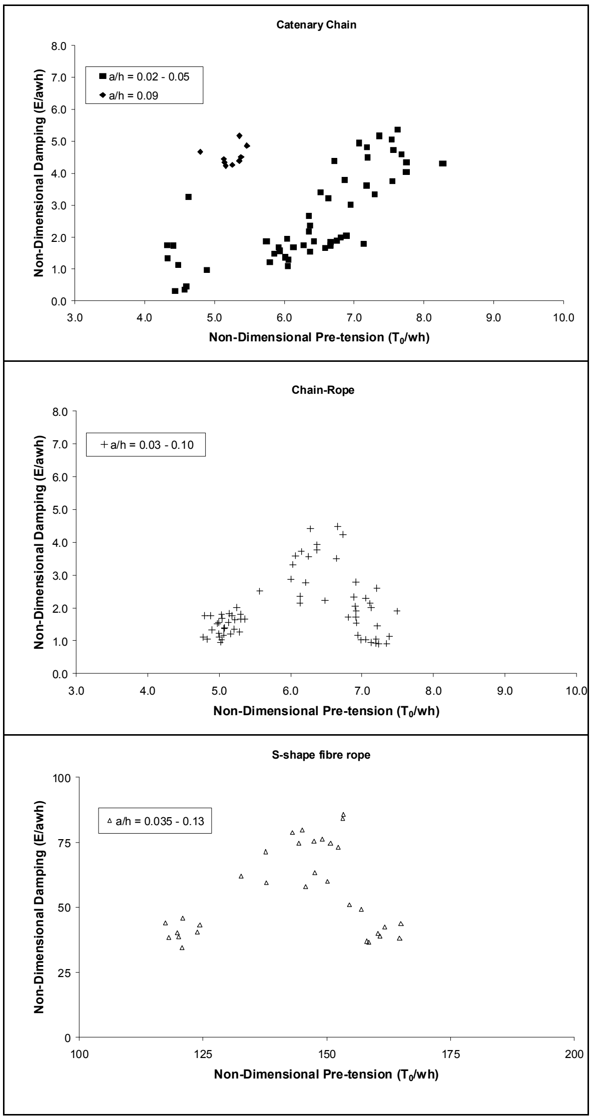

Figure 10a-c Non-dimensional line damping for the line configuration a) catenary chain, b) chain rope and c) S-shape fiber rope (floater sinker).

Comparing the non-dimensional graphs for the three configurations it can be seen that a Gaussian type shape is apparent for the configuration of the chain rope (figure 10b) and S-shape fibre rope (figure 10c), whilst for the chain configuration (figure 10a) this shape cannot be observed. Whilst more data points are included in figure 10a in comparison to figure 8, the maximum non-dimensional pre-tension is similar and hence no statement is possible relating to the Gaussian shape. The observation of a large effect on the mooring line damping due to the amplitude ratio for the chain test at an average value of *a/h* = 0.09, are repeated in figure 10a. The observation of the change in damping behaviour due to variation in amplitude ratio was also observed by Webster [6] during small scale chain experiments.

The observation of a Gaussian type shape for the configurations in figure 10b,c could be contributed to a change in the main damping contributors over the tested pre-tension range.

For the chain-rope configuration (figure 3b) at smaller pre-tension tests sections of the lower chain would rest on the seabed whilst the upper mooring rope would mainly act within a linear tension regime. With increasing pre-tensions the total line configuration would be fully lifted through sections of the sinusoidal motion. This would certainly have an effect on the fluid damping along the line whilst material damping would also be affected. Both, the fluid and material damping would typically contribute to an increase in the overall damping. It is assumed that this is shown in figure 10b for a non-dimensional pre-tension range between T_0/wh = 6.0 – 7.0. For a further increase in damping it might be assumed that fluid damping decreases since the line is close to being fully taut throughout most of the sinusoidal motion. Within this range the sinusoidal motion is mainly due to the stretching characteristics of the fibre rope section. Fluid damping could be assumed to decrease and the main damping contributor would be the material damping characteristics of the rope.

For the S-shape fibre rope similar assumption could be made. However, due to the floater-sinker configuration the main fluid damping would occur at the body of the floater/sinker whilst moving through the fluid. At low pre-tension the motion of the bodies would be relatively slow and hence damping would be small since it is associated to the fluid velocity. Peak damping would most likely be observed once the motion characteristics of these bodies results in fast motions at specific pre-tensions. Once pre-tensions are reached that is close to, or result in a taut line, the motion of the floater/sinker would be minimal and the main damping contribution would be the result of the material damping characteristics.

It might be necessary to illustrate the importance of the variation in non-dimensional amplitude in relation to the different configurations. Lower pre-tensions will allow larger surge motions. For a catenary chain surge motions are restricted by the restoring force due to the increase in weight of the chain as it becomes lifted. Once the chain is fully lifted further restoring forces are given through the anchor holding capacity. At this point motions become very restricted for the catenary chain since the stretching characteristics are small. For the hybrid chain rope configuration the stretching of the upper rope section will always contribute to the surge, allowing larger amplitudes even after the line is fully lifted. Considering the floater sinker configuration the amplitude variation is dependent on the length of the individual sections between anchor, floater, sinker and fairlead, as well as to the stretching characteristics of the rope material.

Taking in consideration the connection between the pre-tension and the associated surge motion, an attempt was made to present the damping result in a more discreet approach. In order to account directly for the connection between surge amplitude *a* and pre-tension T_0 towards the dissipated energy *E*, the results are presented in terms of a non-dimensional damping E/T_0h versus the amplitude ratio *a/h* in figure 11.

All three configurations are presented in figure 11, again identifying separately the group of chain data

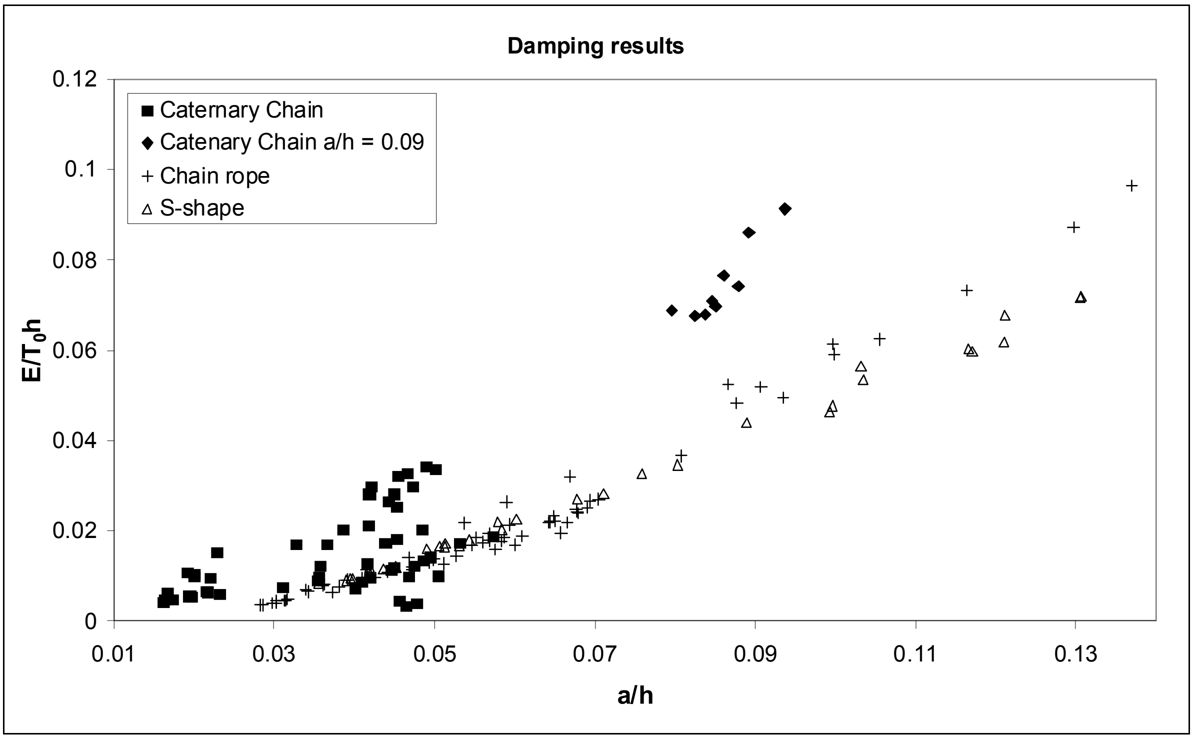

Figure 11 Modified presentation of damping results considering connection between pre-tension and surge amplitude for catenary chain, hybrid chain-rope and S-shape fibre rope.

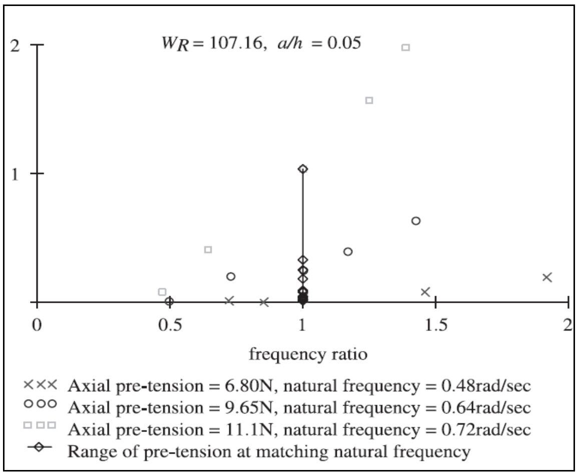

Figure 12 Frequency dependency of the sinusoidal motion towards the damping, Johanning et.al. [7].

points with an average value of *a/h* = 0.09. A linear trend can be observed for all configurations. A spread or scattering within the linear trend can be observed for the catenary chain within the amplitude ratio range of a/h = 0.03 to 0.05. However, if this scattering would be disregarded it could be argued that the catenary chain configuration follows the similar trend as the other two configurations. From figure 11 it can be observed that the catenary chain damping is affected more by the surge amplitude. The damping results for the other two configurations are below that of the catenary chain and are not affected by any anomalies. It could be argued that the chain rope configuration has higher damping characteristics compared with the floater sinker configuration, however they are very close to each other. In order to verify that this result and the representation method are valid, further tests would be needed.

3.2 Frequency dependency

The work by Johanning et.al. [7] also illustrated the frequency dependency of the sinusoidal motion towards the damping, using small scale wave tank testing. Figure 12 is a re-plot of their results, which indicates a linear relationship between the frequency of the forced oscillation and the damping. The variation in frequency was expressed in a non-dimensional ratio between the forced angular velocity, ω_f presented over the natural angular velocity, ω_n,

$$\omega_{ratio} = \frac{\omega_f}{\omega_n} \qquad (3)$$

In the large scale tests an attempt was made to reproduce these findings. The natural frequency for were obtained from transient tests as described above, and tests undertaken at forcing frequencies above and below these values for each pre-tension. The natural periods for the individual oscillatory tests are given in table 2.

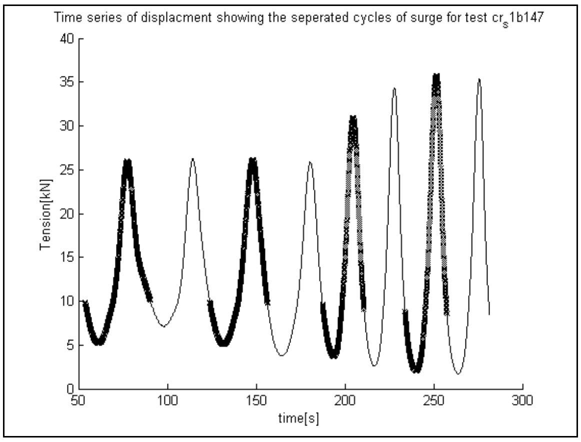

Figure 13 Large scale frequency dependency test

Figure 13 shows a time history of an attempt to vary forced oscillation frequency below and above the natural frequency for a given pre-tension of T_0 = 14.9kN. Again, the control of the vessel made it difficult to obtain precise forced vibrations. It can be observed from the time history in figure 13 that the frequency variation has a direct affect on the tension variation. For oscillatory vessel motions at lower frequencies smaller peak tension were measured, whilst higher frequency oscillations resulted in larger peak tensions.

Applying the same methodology, as used by Johanning et.al. [7], by presenting the non-dimensional damping versus the frequency ratio, a similar linear relationship can be observed for the large scale test (figure 14). This affect could be attributed to the difference in velocity change for the frequency oscillations that has an affect on the fluid damping. However, no detailed conclusion can be made at this stage.

4 Discussion

The detailed analysis of the damping behaviour for three mooring configurations, namely a catenary chain, hybrid chain-rope and a S-shape fibre rope, identified that the damping behaviour is dependent on i) the configuration, ii) pre-tension, iii) surge amplitude and iv) forced frequency oscillation. Since the experiments were conducted at large scale in real sea conditions anomalies were observed that could not necessarily be quantified. However, observation form these large scale experiments support earlier results conducted in a controllable tank environment by Webster [6] and Johanning et.al. [7].

For the hybrid chain-rope and the S-shape fibre rope configurations a Gaussian type trend was observed when plotting the non-dimensional damping against the non-dimensional pre-tension. This however was not observed for the catenary chain configuration. It is proposed that there is a direct connection between the surge amplitude and pre-tension that has an effect on the damping. It is suggested that in this case, rather than presenting damping in the non-dimensional form often used in

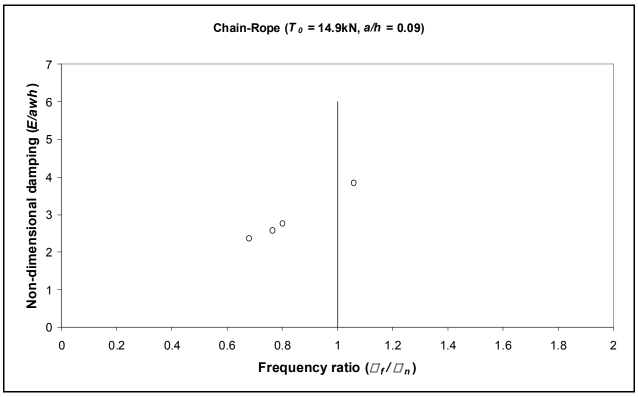

Figure 14 Frequency dependency of sinusoidal motion for large scale test at pre-tension of T_0 = 14.8kN and amplitude ration *a/h* = 0.09 for chain rope configuration.

the literature (E/awh), a new non-dimensional parameter, where the energy dissipation is scaled with respect to the pre-tension and water depth *(E/T_{0h})*. It was found that the presentation of the latter non-dimensional damping plotted against the surge amplitude ratio *(a/h)* resulted in a linear trend. This, however, needs validation through detailed controllable small scale tests and this will be part continuing research within the group.

Finally the investigation of frequency dependency towards the damping behaviour at large scale, using only hybrid chain-rope results, confirmed a tendency similar to that observed during small scale test performed by Johanning et.al. [7]. The trend of a linear change in damping behaviour was observed for a single pre-tension when plotted against the frequency ratio (ω_f / ω_n).

Considering the controllability issues experienced during the large scale experiments the results are satisfactory. However, confirmation of some of the outcomes should be obtained through controlled tank tests, taking scaling issues into consideration.

Acknowledgements

The authors would like to acknowledge of the Engineering and Physical Science Research Council for its support, through the SUPERGEN marine energy research consortium. The first author would like to express his thanks especially to the EPSRC for providing him with a PhD scholarship through the SuperGen Marine DTP in marine energy research.

References

[1] Huse, E. (1991); New Development in Prediction of Mooring Line Damping, 23th Offshore Technology Conference, OTC 6593, May 6-9, 1991, Houston, Texas, USA

[2] Bauduin, C. and Naciri, M. (2000) A contribution on quasistaticmooring line damping, Journal of the Offshore Mechanics and Arctic Engineering, OMAE, Vol. 122, p. 125-133

[3] Hamilton, J. and Kitney, N. (2004) An alternative mooringline damping methodology for deep water, Proceeding of the 14thInt. Offshore and Polar Engineering Conference, ISOPE, 23-28.05.2004, Toulon, France

[4] Huse, E. (1986); Influence of mooring line damping uponrig motion, 18th Offshore Technology Conference, OTC 5204,May 5-8, 1986, Houston, Texas, USA

[5] Liu, Y. and Bergdahl, L. (1998) Improvement on Huse'smodel for estimating mooring cable induced damping, Proceedingof the 17th Offshore Mechanics and Arctic Engineering, OMAE

[6] Webster, W.C. (1995), Mooring-induced damping, Ocean Engineering, Vol. 22, No. 6, pp. 571-591

[7] Johanning L, Smith GH and Wolfram J. (2007). Measurements of static and dynamic mooring line damping and their importance for floating WEC devices. Ocean Engineering 34(14–15): 1918–1934.

[8] Johanning, L., Smith, G. H. and Wolfram, J. (2006), Mooring design approach for Wave Energy Converter, Proceedings of the Institution of Mechanical Engineers, Part M, Journal of Engineering for the Maritime Environment (JEME)220,Part M:pp 159-174

[9] L Johanning and GH Smith.(2008) Station keeping study for WEC devices including compliant chain, compliant hybrid and taut arrangement. 27th Int.Conference on Offshore Mechanics and Arctic Engineering(OMAE), No. OMAE2008-57184, 15.-20.06,2008, Estoril, Portugal

[10] Johanning, L., Smith, G.H. and Bullen C. (2007) Large scale mooring line experiments and comparison with a fully dynamic simulation program with importance to WEC installation, 17th Int. Offshore (Ocean) and Polar Engineering Conference, ISOPE, 01. - 06.07.2007, Lisbon, Portugal

[11] L Johanning and GH Smith. Improved measurement technologies for floating wave energy converter mooring arrangements. International Journal of the Society for Underwater Technology, 27,N.o4:1–10, 2008.

[12] L. Johanning AND G.H. Smith; Comparison of simulation and test results for a generic moored WEC using a catenary mooring arrangement, International conference OCEAN ENERGY, OTTI, 23.10 – 24.10.2006, Bremerhaven, Germany